

An attic-interior infiltration and interzone transport model of a house

I.S. Walker^a, T.W. Forest^{b,*}, D.J. Wilson^b

^aLawrence Berkley Laboratory, Berkeley, CA, USA

^bDepartment of Mechanical Engineering, University of Alberta, Edmonton, Alta., Canada T6G 2G8

Received 16 July 2002; accepted 29 June 2004

Abstract

A detailed model is developed for predicting the ventilation rates of the indoor, conditioned zone of a house and the attic zone. The complete set of algorithms is presented in a form for direct incorporation in a two zone ventilation model. One of the important predictions from this model is the leakage flow rate between the indoor and attic zones. Ventilation rates are predicted from a steady state mass flow rate balance for each zone where all individual flow rates through leakage sites are based on a power law expression for flow rate versus pressure difference. The envelope leakage includes distributed leakage associated with background leakage, localized leakage associated with vents and flues, and active fan ventilation. The predicted ventilation rates agree quite well with field measurements of ventilation rates in houses and attics with different leakage configurations, without the use of any empirically adjusted parameters or constants.

© 2004 Elsevier Ltd. All rights reserved.

Keywords: Attic; House; Infiltration; Ventilation; Wind; Buoyancy; Tracer gas

1. Introduction

Ventilation is generally classified as passive (relying only on natural driving forces of wind and indoor–outdoor temperature difference) or active (operation of an exhaust fan). For the indoor, conditioned zone, ventilation is used to remove indoor air contaminants such as volatile organic compounds, radon gas, and excess moisture. For unconditioned zones such as attics, ventilation is used to control excessive temperatures and moisture accumulation. A detailed description of previous studies of attic ventilation is given by Walker and Forest [1].

Since ventilation plays such a large role in controlling the interior environment of a house, it is important that simple and reliable models be developed to predict ventilation rates based on meteorological conditions and characteristics of the leakage area of the building

envelope. Ventilation models by the authors and other co-workers have considered a single indoor zone with distributed leakage [2,3]. Single zone models have been extended to include localized leakage associated with large openings such as, vents and furnace flues [4]. In these models, the individual mass flow rate through each leakage site is calculated based on the pressure difference acting at the leakage site and the flow characteristic of the leakage site. This pressure difference is a combination of the actions of wind and indoor–outdoor temperature difference. The superposition of these two pressure differences is discussed by Walker and Wilson [5]. For the attic zone, Forest and Walker [6] describe a ventilation model based on the same approach taken by Walker and Wilson [4], which includes background leakage of the attic envelope and localized leaks associated with roof vents. A simplified version of this attic ventilation model is presented in Walker et al. [7] for use as a diagnostic tool.

The present work was undertaken to develop a two zone model to predict ventilation rates in a given zone as well as the mass flow rate between the zones. Our focus

*Corresponding author. Tel.: +1-780-492-2675; fax: +1-780-492-2200.

E-mail address: tom.forest@ualberta.ca (T.W. Forest).

here is on the attic zone. The inter-zonal house-to-attic leakage flow rate is important since this flow convects both heat and moisture into the attic zone. The two zone ventilation model developed here falls between extremely complex multi-zone models such as, Feustal and Raynor-Hoosen [8] which require a great deal of input data that is difficult to determine and simple single zone ventilation models. The predictions of zone ventilation rates and the inter-zonal flow rate are compared with measurements of these rates at the Alberta Home Heating Test Facility over several years of testing and for houses with different leakage configurations. The predicted rates will be shown to agree quite well with measured values without recourse to empirically adjusted parameters or constants.

2. Attic-interior two zone ventilation model

In order to develop a model for predicting attic ventilation rates, the house that is being modeled is divided into two zones: a single interior zone that is conditioned to some constant temperature, and an attic zone that is not conditioned. Both zones are included in the ventilation model since one of the important predictions from the model is the inter-zonal leakage flow rate; this leakage air flow can convect moisture into the attic space where condensation occurs during periods of cold weather. One of the important features of our ventilation model is the combination of distributed leakage area with site-specific, localized leaks such as, attic vents, soffits, combustion air inlets, and furnace flues. Walker and Wilson [4] have shown how including a single localized leak (in their case a furnace flue) can have a significant effect on calculated ventilation rates in a model with distributed leaks.

We consider a residential building that has a rectangular plan form as shown in Fig. 1. The plan form is restricted to rectangular shapes where the longest side is no more than about three times the shorter side because wall pressure coefficients used in calculating wind pressures (see Section 2b) have been taken from data sets that are restricted to these simple shapes. The attic is restricted to having two pitched surfaces with gable ends. This restriction is set by the availability of measured data for roof pressure coefficients rather than any real “typical” roof construction. More complex building shapes can be incorporated in the model if data on surface pressure coefficients exists. The air in the two zones is assumed to be well-mixed implying that air has uniform properties within each zone although these will be different in the two zones. The interior zone is assumed to be at a constant, specified temperature while the attic air temperature is dependent on meteorological conditions including solar gain, ventilation rate, and attic insulation level. In our

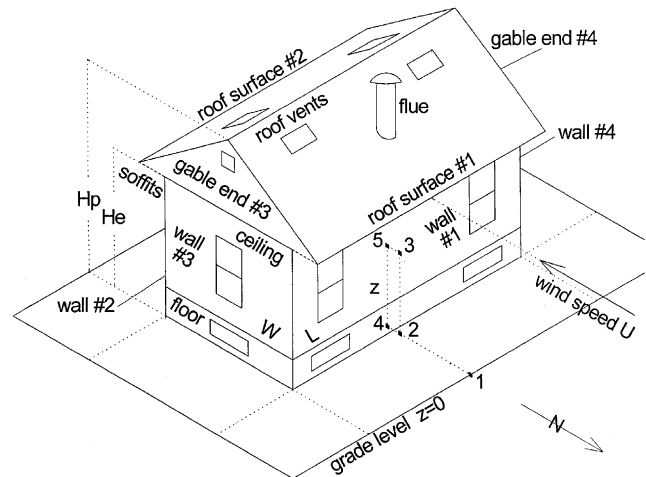


Fig. 1. Schematic of house showing reference numbers for wall and roof surfaces and reference numbers for points on the building envelope where pressures are calculated.

comparison of measured and predicted attic ventilation rates given in Section 3, we used the measured attic air temperatures rather than values predicted by an attic thermal model. An attic thermal model is beyond the scope of this paper. In connection with the assumption of well-mixed zones, it is further assumed that there are no vertical temperature gradients either inside each zone or outdoors. Measurements performed in our test houses by Dale and Ackerman [9] have shown that this is a good assumption because all the change in temperature in indoor air occurs in thin boundary layers on the walls, the floor and the ceiling that are about 5% or less of the total room volume. Furthermore, it is assumed that the density and viscosity of air depend only on temperature.

The building envelope leakage is divided into three categories: *distributed* leakage which includes all small cracks, holes, and imperfections in the envelope, *localized* leakage sites such as, furnace flues and attic vents, and *active* leakage sites with fans. Fans are included using a fan pressure-flow performance curve so that if large natural pressures due to wind and stack effect occur at the fan location then the fan flow will change. The distributed leakage area is assumed to be spread uniformly over each wall and roof surface with the flow characteristics independent of the flow direction. The general mass flow rate equation for each localized leak is assumed to be

$$\dot{m} = \rho C \Delta P^n, \quad (1)$$

where \dot{m} is mass flow rate (kg/s), ρ is the density of air (kg/m³), C is the leakage flow coefficient (m³/(sPaⁿ)), ΔP is the pressure difference across the leak (Pa), and n is the flow exponent. The value of n varies from 1.0 for laminar flow to 0.5 for turbulent orifice flow. Values of C and n are obtained from separate measurements of

flow rate as a function of ΔP ; in the case of distributed leakage area, C and n are obtained from pressurization tests on the interior zone or attic. The flow direction is determined by ΔP where a positive ΔP produces inflow (infiltration) and a negative ΔP produces outflow (exfiltration). A density and viscosity correction factor is applied to C for building and attic leaks to account for changes in air temperature. Kiel et al. [10] used dimensional analysis of flow in a short crack to show that

$$C \propto \frac{\rho^{n-1}}{\mu^{2n-1}}, \quad (2)$$

where μ is the dynamic viscosity of air. To make this relationship easier to implement in the ventilation model it is assumed that over the range of temperatures encountered in model predictions, the viscosity of air is a linear function of temperature only. Neglecting the effect of varying atmospheric pressure, Eq. (2) can be expressed in terms of temperature as

$$C = C_{\text{ref}} \left(\frac{T}{T_{\text{ref}}} \right)^{3n-2}, \quad (3)$$

where T is the absolute temperature at which C is calculated. For many interior zones and attics, the distributed background leakage has $n \sim 0.67$ which implies in Eq. (3) that there is no temperature correction to C . For simplicity, our model does not apply any temperature correction for distributed leakage. For localized leaks n is typically 0.5, which is characteristic of fully turbulent flow and temperature corrections to C can be significant.

2.1. Pressure difference across the building envelope

The pressures driving flows through the leak result from the surface pressures due to wind acting on the building combined with buoyancy pressure induced by density differences caused by temperature differences between indoor and outdoor air. In the ventilation model, the pressures resulting from the two effects are calculated separately, and then added linearly to predict the pressure difference across the building envelope at any point.

We first consider the effect of wind on a building. To find the outside pressure on a given surface of the house or attic, a wind pressure coefficient, C_P , is used that includes a wind speed multiplier, S_U to account for shelter; specific values for C_P and S_U are given in Sections 2c and 2d below. The wind speed, U , is referenced to the eave height of buildings. This wind speed is used because the pressure coefficients taken from wind tunnel studies are normalized by the eave height wind speed. All wind pressure coefficients are averaged over a given surface; thus, extremes of wind

pressure occurring for example, at corner flow separation regions, are not accounted for in the model. Different sets of pressure coefficients are used for houses in a row as compared to a single house to account for the different flow patterns around a row of houses versus a single house. The following equation is used to calculate the pressure difference due to wind effect:

$$\Delta P_U = \rho_{\text{out}} C_P \frac{(S_U U)^2}{2}, \quad (4)$$

where ΔP_U is the difference between the pressure on the surface of the building due to the wind and the atmospheric reference pressure, P_∞ far away from the building where the building does not influence the flow field, and is at grade (i.e. ground) level as opposed to eave height (point 1 in Fig. 1). The outdoor air density, ρ_{out} is chosen as the reference density for calculating surface pressures because pressure coefficients are measured in terms of the external ambient conditions. The shelter coefficient, S_U accounts for wind speed reductions due to upwind obstacles that shelter a building; a shelter coefficient of $S_U = 1.0$ implies no shelter and $S_U = 0$ implies complete shelter resulting in no wind effect. Because each leak has a different pressure and shelter coefficient it is convenient to define a reference wind pressure P_U as

$$P_U \equiv \rho_{\text{out}} \frac{U^2}{2}. \quad (5)$$

Eq. (4) can then be written in terms of P_U :

$$\Delta P_U = C_P S_U^2 P_U. \quad (6)$$

This definition of P_U will be used later in the equations for the flow through each leak.

The air pressure inside and outside the house varies with elevation, z (referenced to ground level, $z = 0$) due to the hydrostatic gradient, which depends on the density of the air. Since air density depends on temperature, a pressure difference is generated across a building envelope due to the different air temperature inside and outside the zone. This component of pressure difference is referred to as the “stack” effect. The variation in pressure with z is given by

$$P = P_{z=0} - \rho g z, \quad (7)$$

where $P_{z=0}$ is the pressure at grade level (Pa), and g is the gravitational acceleration (m/s^2).

The combined wind and stack pressure difference across the building envelope, ΔP at any elevation, z is defined as the outdoor minus the indoor pressure. Consider some arbitrary point 3 on the outside of the house as shown in Fig. 1. The pressure at this point is

$$P_3 = P_2 - \rho_{\text{out}} g z. \quad (8)$$

The grade level pressure, P_2 differs from the atmospheric pressure far away from the house (P_∞ at point 1)

due to the wind pressure as given by Eq. (6). Thus, P_3 becomes

$$P_3 = P_\infty + C_P S_U^2 P_U - \rho_{out} g z. \tag{9}$$

For the interior of the house there is no wind pressure effect and the pressure at the interior point 5 corresponding to point 3 is

$$P_5 = P_4 - \rho_{in} g z, \tag{10}$$

where P_4 is the reference pressure at ground level inside the house. Thus, the combined wind and stack pressure difference across the building envelope at any elevation, z becomes

$$\Delta P \equiv P_3 - P_5 = (P_\infty - P_4) + C_P S_U^2 P_U - z P_{Tin}, \tag{11}$$

where P_{Tin} is defined as the outdoor–indoor pressure gradient

$$P_{Tin} \equiv g \rho_{out} \left(\frac{T_{in} - T_{out}}{T_{in}} \right). \tag{12}$$

The term $P_\infty - P_4$ in Eq. (11) is a reference pressure difference, which we will denote as P_{Rin} .

Eq. (11) gives the combined wind and stack pressure difference at any point on the building envelope for the interior zone where the temperature is T_{in} . If we consider the attic zone where the temperature is T_a , the expression for the combined pressure difference across the attic envelope at any elevation, z is

$$\Delta P = P_{Ra} + C_P S_U^2 P_U - z P_{Ta}, \tag{13}$$

where the outdoor–indoor pressure gradient factor, P_{Ta} is defined by Eq. (12) with T_{in} replaced by T_a . Note that the term P_{Ra} is the reference outdoor–indoor pressure difference at ground level for the attic zone and is based on a fictitious interior zone temperature of T_a instead of T_{in} . This term is not the same as the ground level reference pressure difference, P_{Rin} corresponding to the interior zone. The reference pressure difference for the interior and attic zones are calculated from a steady state mass flow rate balance on each zone. The mass flow rate solution technique is described in Section 2f.

Eqs. (11) and (13) are applied to each leak for the interior and attic zones with the appropriate values of C_P , S_U and z . The linear change in pressure, ΔP , with height, z , due to the stack effect term in Eqs. (11) and (13) means that when inflows and outflows are balanced, there is a neutral level location, H_{NL} on each building envelope surface where there is no pressure difference. For the interior zone, when T_{in} is greater than T_{out} flow is in below H_{NLin} and out above H_{NLin} , and the flow directions are reversed when T_{in} is less than T_{out} . In general the neutral level is different for each wall because wind pressures can drive H_{NLin} above the ceiling or below the floor. In those cases there is one-way flow through the wall. The neutral level for surface, i of the interior zone is found by setting ΔP equal to 0 in

Eq. (11) and solving for $z = H_{NLin,i}$:

$$H_{NLin,i} = \left(\frac{P_{Rin} + C_{P,i} S_{U,i}^2 P_U}{P_{Tin}} \right). \tag{14}$$

Similarly, for the attic zone, the neutral level, $H_{NLa,i}$ for any surface, i is

$$H_{NLa,i} = \left(\frac{P_{Ra} + C_{P,i} S_{U,i}^2 P_U}{P_{Ta}} \right). \tag{15}$$

2.2. Wind pressure coefficients for vertical walls and sloped roofs

In order to calculate the pressure produced by the action of wind on a building, wind pressure coefficients for this model are taken from wind tunnel tests. As mentioned previously, wind pressure coefficients used in this model are averaged over a given surface. The wind pressure coefficients depend on wind direction and are expressed in the ventilation model as a continuous function of wind angle. Walker and Wilson [11,12] discuss these effects in greater detail. For the vertical walls of a house, Table 1 contains the wall-averaged wind pressure coefficients used in the ventilation model for wind perpendicular to the upwind wall. The values given in Table 1 are based on the cited authors' interpretation of data taken over a wide range of experimental conditions. For a closely spaced row of houses, the wind is blowing along the row of houses. When the wind is not normal to the upwind wall these pressure coefficients do not apply. An empirical trigonometric function was developed in the present study to interpolate between these normal values to fit the data given in Table 1. For each wall of the building the harmonic function for C_p is

$$C_p(\theta) = \frac{1}{2} \{ [C_p(1) + C_p(2)] \cos^{1/2} \theta + [C_p(1) - C_p(2)] \cos^{3/4} \theta + [C_p(3) + C_p(4)] \sin^4 \theta + [C_p(3) - C_p(4)] \sin \theta \}, \tag{16}$$

where the pressure coefficients $C_p(1)$ refers to the upwind wall in Table 1 (+0.60), $C_p(2)$ refers to the

Table 1
Wall averaged wind pressure coefficients, C_p for a rectangular building with the wind normal to upwind wall from Akins et al. [13] and Wiren [14]

House configuration	Wall pressure coefficient, C_p		
	Upwind wall	Side walls	Downwind wall
Isolated house	+0.60	-0.65	-0.3
In-line closely-spaced row	+0.60	-0.2	-0.3

downwind wall 180° (−0.3), C_p (3) refers to the east side wall (−0.65 or −0.2), and C_p (4) refers to the west side wall (−0.65 or −0.2); θ is the angle measured clockwise between the normal to wall under consideration and the wind direction. This function is shown in Fig. 2 together with data from Akins et al. [13] for a cube. The error bars on the data points in Fig. 2 represent the uncertainty in reading the measured values from the figures of Akins et al. Eq. (10) fits the measured data to within ± 0.02 except at approximately 150° and 210° (which are the same by symmetry) where the equation overpredicts the pressure coefficient by about 0.1.

For the attic zone, the model has been developed for a gable end attic with two sloped roof surfaces. The pressure coefficients for gable ends or soffits are assumed to be the same as those on the walls below them and are calculated using the same procedure as for the house walls. The sloped roof surfaces have pressure coefficients that are also a function of roof slope. Table 2 gives values of C_p measured by Wiren [14] for upwind and downwind sloped roof surfaces with wind normal to the upwind surface for different roof slopes. For a flat roof both surfaces are in a separation zone and experience large negative pressures. Steeper roofs of higher slope have some stagnation on the upwind

surface but still have negative pressure coefficients for the downwind surface in the separation zone. The roof pressure coefficients are averaged over the entire sloped roof surface. For wind flow parallel to the roof ridge, the pressure coefficients change in the same way as for houses with C_p equal to −0.6 for an isolated building and C_p equal to −0.2 for row houses for both sloped roof surfaces. The pressure coefficient is independent of roof pitch for flow parallel to the roof ridge.

To account for the variation of roof pressure coefficients with wind angle a similar empirical relationship to that for walls (Eq. (16)) has been developed for this study. For each roof surface:

$$C_p(\theta) = \frac{1}{2} \{ [C_p(1) + C_p(2)] \cos^2 \theta + [C_p(1) - C_p(2)] F(\theta, \psi) + [C_p(3) + C_p(4)] \sin^2 \theta + [C_p(3) - C_p(4)] \sin \theta \}, \quad (17)$$

where the pressure coefficients $C_p(1)$ refers to the upwind roof surface in Table 2, $C_p(2)$ refers to the downwind roof surface, $C_p(3)$ refers to the east gable surface (assumed to be the same value as the east side wall below the gable end), and $C_p(4)$ refers to the west gable surface (assumed to be the same value as the west side wall below the gable end); as with the wall pressure coefficients, θ is the angle measured clockwise from the horizontal component of the normal to roof surface 1 and the wind direction. $F(\theta, \psi)$ is a switching function to account for changes in roof slope. To include the change of C_p with different roof slopes shown in Table 2, the empirical switching function, F is expressed as

$$F(\theta, \psi) = \frac{1 - (|\cos \theta|)^5 \left(\frac{28 - \psi}{28} \right)^{0.01}}{2} + \frac{1 + (|\cos \theta|)^5}{2}, \quad (18)$$

where ψ is the roof slope in degrees, measured from the horizontal. Eq. (18) acts like a switch with $F \sim 1$ for ψ between 0° and 28° and $F \sim \cos \theta$ when ψ is greater than 28°. The switch point of 28° is chosen so that this relationship produces the same results as in Table 2. Eq. (18) is not used to change the pressure coefficients shown in Table 2, but it changes the functional form of Eq. (17) so that the interpolation fits the measured pressure coefficients. Eq. (17) is compared with sloped roof pressure coefficients from Liddament [15] in Figs. 3–5 for roof slopes, ψ greater than 30°, 10°–30°, and less than 10°, respectively. In each case the equation fits the data well, typically within ± 0.01 . The exception is for ψ greater than 30° at wind directions of 45° and 315° (the same by symmetry) where the maximum difference between the interpolated and measured pressure coefficients is 0.1.

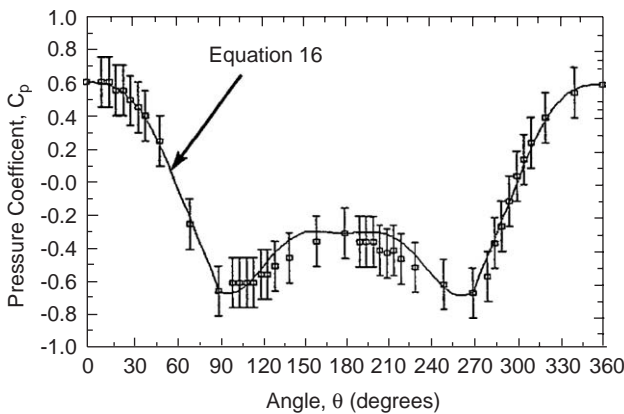


Fig. 2. Wind angle dependence of measured [13] and predicted wall pressure coefficients for isolated buildings; θ is the angle between the wall normal and the wind direction measured clockwise.

Table 2
Sloped roof average wind pressure coefficients, C_p for wind normal to the upwind surface [14]

Roof pitch	Wind pressure coefficient, C_p	
	Upwind surface	Downwind surface
<10°	−0.8	−0.4
10°–30°	−0.4	−0.4
>30°	+0.3	−0.5

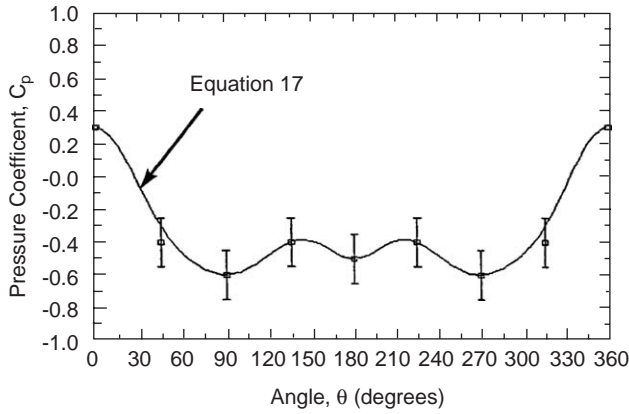


Fig. 3. Wind angle dependence of measured [15] and predicted surface pressure coefficients on a sloped roof surface for a roof slope greater than 30°; θ is the angle between the wall normal and the wind direction measured clockwise.

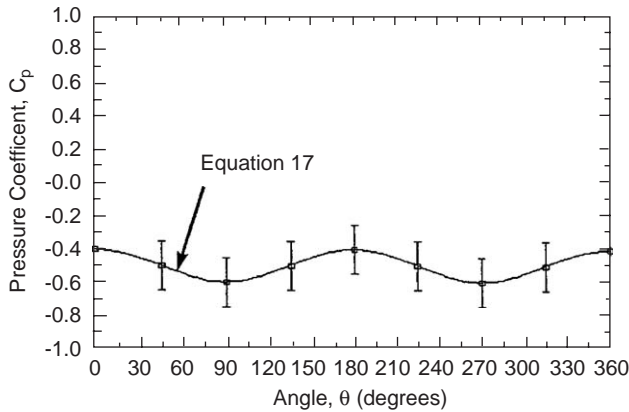


Fig. 4. Wind angle dependence of measured [15] and predicted surface pressure coefficients on a sloped roof surface for a roof slope of 20°; θ is the angle between the wall normal and the wind direction measured clockwise.

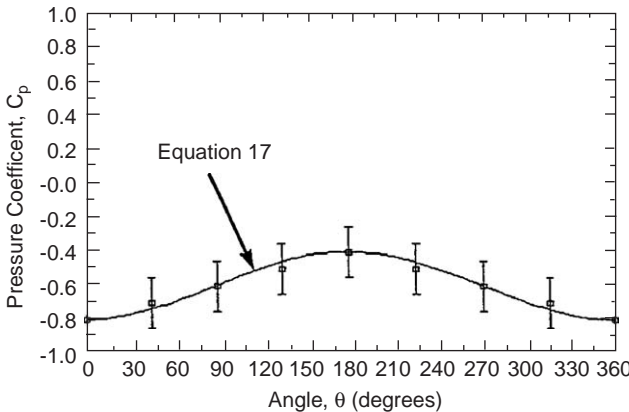


Fig. 5. Wind angle dependence of measured [15] and predicted surface pressure coefficients on a sloped roof surface for a roof slope of less than 10°; θ is the angle between the wall normal and the wind direction measured clockwise.

2.3. Wind shelter

Local wind shelter provided by other buildings, trees, fences, bushes etc. has a significant effect on the surface pressures that affect house ventilation but is difficult to quantify. Ventilation rates measured for the present study have shown reductions in ventilation rates of up to 300% when the wind changed direction from perpendicular to parallel to the row of test houses. Some of these results have been reported in Wilson and Walker [16]. Previous ventilation models have included shelter in broad classes with sharp changes from class to class. For example, Sherman and Grimsrud [2] used a look-up table with five classes of shelter described in words such as “Light local shielding with few obstructions”. This shelter was assumed to be the same for all wind directions.

In our ventilation model shelter effects are separated from the effects of changing pressure coefficients with wind direction. The shelter coefficient, S_U , acts to reduce the unsheltered wind speed so that an effective wind speed, U_S can be defined as

$$U_S = S_U U, \tag{19}$$

where U is the wind speed at eave height with no building and no sheltering effects. The shelter coefficient has the limits of $S_U = 1.0$ that implies no shelter and $S_U = 0$ that implies total shelter with no wind pressure on the wall. Note that U_S is not necessarily the wind speed that would be measured by an anemometer in the wake of the object that is sheltering the house, but instead is the effective speed for finding the surface pressures. As will be shown later, the coefficients used to find U_S from S_U are based on measured pressures not velocities. Here we will summarize two methods for estimating wind shelter. The first method can be used if little is known about the surrounding obstacles. The second “wind-shadow” method is much more sophisticated and provides estimates of shelter based on the geometry of the surrounding obstacles.

The first method simply provides an interpolation function and requires estimates of shelter to be made for winds perpendicular to the four sides of the building [16]. This interpolation function has the same form as Eq. (16) so that for each wall

$$S_U = \frac{1}{2} \{ [S_U(1) + S_U(2)] \cos^2 \theta + [S_U(1) - S_U(2)] \cos \theta + [S_U(3) + S_U(4)] \sin^2 \theta + [S_U(3) - S_U(4)] \sin \theta \}, \tag{20}$$

where the shelter coefficients, $S_U(1)$ refers to the upwind wall, $S_U(2)$ refers to the downwind wall, $S_U(3)$ refers to the east side wall, and $S_U(4)$ refers to the west side wall; θ is defined in the same manner as in Eq. (16). This

method of calculating wind shelter may be used when little is known about the building site.

In the second method, to improve shelter estimates a wind-shadow shelter method was developed to calculate numerical values for the reduction in velocity caused by an upwind obstacle. The wind-shadow method is discussed in greater detail in Walker and Wilson [12]. This method can be used when more detail about building and site geometry is known, and this wind-shadow approach is used in the model validations presented later. The shelter factor, S_U is

$$S_U = 1 - \left(\frac{3.3}{\frac{s}{R_B} + 3.3} \right)^{3/2}, \quad (21)$$

where s is the separation distance between the obstacle and the building measured along the wind direction. The characteristic building dimension, R_B , was defined by Wilson [17] as

$$R_B = D_Y^{2/3} D_L^{1/3}, \quad (22)$$

where D_Y is the smallest building dimension and D_L is the largest building dimension of projected width or projected height. For the validation of the ventilation model a computer program was used to calculate S_U for all four walls of the test buildings at The Alberta Home Heating Test Facility every 1° of wind angle. An example variation of S_U with wind direction is illustrated in Fig. 6.

2.4. Calculation of air flows across the attic envelope

The total leakage associated with the interior or attic zones is divided into distributed leakage (i.e. all the small cracks and imperfections in the envelope) and localized leakage (i.e. all identifiable leaks such as vents

and flues). The flow through each leak is calculated using the pressure difference across each leak as given by Eqs. (11) and (13), respectively, and the mass flow rate given by Eq. (1). We will develop expressions for mass flow rates for the attic zone first and then summarize these for the interior zone. In principal, the two zones are treated in an identical fashion. The development of the steady state mass flow rate balance follows that given by Forest and Walker [6] for attic zones but includes the important coupling between the two zones, which produces an interior-attic exchange mass flow rate. In Section 2f we discuss how this exchange flow rate is calculated.

We first consider the total air flow through the distributed leakage in the attic envelope. It is assumed that the total distributed leakage flow coefficient $C_{d,a}$ and exponent n_a are known from fan pressurization results for the attic envelope; it is also assumed that all distributed leakage sites have the same flow exponent. The flow coefficients for the sloped roof surfaces and soffits must be estimated as fractions of the total distributed leakage such that

$$C_{d,a} = \sum_{i=1}^4 C_{s,i} + C_r, \quad (23)$$

where C_r is the total leakage in the two pitched roof surfaces and $C_{s,i}$ is the leakage in the soffit or gable ends above each wall surface, i . For the attics tested in this study the north and south sides have soffits and the east and west sides have gable ends as shown in Fig. 1. The soffits are referenced to wall Sections 1 and 2 since they are assumed to have the same wind pressure coefficients as that associated with the vertical wall below the soffits. The two sloped roof surfaces are assumed to have equal leakage; therefore, the flow coefficient for each roof surface is $0.5 C_r$.

The pressure coefficients, C_p for the sloped roof surfaces are obtained from Eq. (11) and Table 2. The sloped roof is assumed to have the same shelter factor as the furnace flue. This means that if the surrounding obstacles are not as high as the flue top (which is close to roof peak height as shown in Fig. 1) then the sloped roof surfaces have no shelter and S_U is equal to 1. If the surrounding obstacles are higher than the flue top then the shelter coefficient, S_U for the sloped roof surfaces is estimated to be the same as that of the wall below them. For example, a south facing roof surface would have the same shelter coefficient as calculated for the south facing wall below it. For the sloped roof surfaces, the neutral level, $H_{NL,a}$, is calculated for the two roof surfaces using the appropriate values of C_p and S_U in Eq. (15).

The change in attic envelope pressure difference with height, z , on the roof surfaces as given by Eq. (13) implies that the flow through the roof is a function of height. The total mass flow rate associated with the

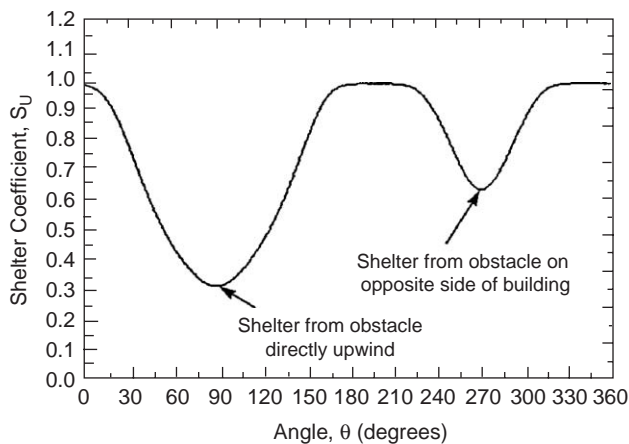


Fig. 6. Wind angle dependence of the shelter coefficient, S_U for the east wall of a house at the Alberta Home Heating Research Facility. Shelter coefficients are calculated using the data of Wiren [14] and the wind-shadow method.

distributed leakage on each roof surface is obtained by integrating the pressure difference over the height of the attic. Consider a differential element of height, dz at any elevation, z on the attic envelope. The differential leakage coefficient, $dC_{r,i}$ associated with this element is

$$dC_{r,i} = C_{r,i} \frac{dz}{(H_p - H_e)}, \quad (24)$$

where H_p and H_e are the heights of the roof peak and eaves measured from grade level, respectively. Using Eq. (1) the differential mass flow rate associated with this element is

$$d\dot{m}_{r,i} = \rho \Delta P^{n_a} dC_{r,i}, \quad (25)$$

where ΔP is given by Eq. (13) and the air density is evaluated at T_{out} for inflow and at T_a for outflow. Substituting Eq. (24) in Eq. (25) and integrating gives an expression for the mass flow rate associated with the distributed leakage on roof surface, i :

$$\dot{m}_{r,i} = \frac{\rho C_{r,i}}{(H_p - H_e)} \int \Delta P^{n_a} dz, \quad (26)$$

where the limits of integration depend on the neutral level, $H_{NLa,i}$ given by Eq. (15). When the attic temperature is greater than the outdoor temperature and $H_{NLa,i}$ is located somewhere on the roof surface, i there is inflow below the neutral level and outflow above the neutral level and these mass flow rates are calculated separately. The mass flow rate associated with the inflow, $\dot{m}_{ri,in}$ is obtained by integrating Eq. (26) from H_e to $H_{NLa,i}$:

$$\dot{m}_{ri,in} = \frac{\rho_{out} C_{r,i} \Delta P_{e,i}^{n_a+1}}{(H_p - H_e)(n_a + 1)P_{Ta}}, \quad (27)$$

where $\Delta P_{e,i}$ is the eave height pressure difference given by Eq. (13) with z equal to H_e . Similarly, the outflow, $\dot{m}_{ri,out}$ is obtained by integrating Eq. (26) from $H_{NLa,i}$ to H_p :

$$\dot{m}_{ri,out} = \frac{\rho_a C_{r,i} \Delta P_{p,i}^{n_a+1}}{(H_p - H_e)(n_a + 1)P_{Ta}}, \quad (28)$$

where $\Delta P_{p,i}$ is the peak height pressure difference given by Eq. (13) with z equal to H_p . If the attic air temperature is less than the outdoor temperature and the neutral level is located somewhere on the roof surface, there is outflow below the neutral level which is given by the expression in Eq. (27) with ρ_{out} replaced by ρ_a . The inflow above the neutral level is given by Eq. (28) with ρ_a replaced by ρ_{out} . For those cases when the neutral level is not located on the roof surface, there is inflow over the entire roof surface when the neutral level is above H_p and outflow when the neutral level is below H_e . The individual mass flow rates are kept separate in order to do the overall mass flow rate balance on each zone.

The mass flow rates through the distributed leakage in the gable end surfaces are treated in the same fashion as the sloped roof surfaces. We assume that the distributed leaks in the gable ends are located at an average height of $1/2(H_p + H_e)$. Thus, the pressure difference across the gable ends is given by Eq. (13) with z equal to the average height; the pressure and shelter coefficients for each gable end surface is assumed to be the same as the wall below the gable end. As mentioned previously, the gable end leakage coefficients, $C_{s,3}$ and $C_{s,4}$ are estimated as fractions of the total attic distributed leakage coefficient. The mass flow rate is then given by Eq. (1) with the gable end pressure difference and leakage flow coefficient. Whether the flow is into the attic or out of the attic will depend on the neutral level for each gable end surface as given by Eq. (15). For the soffits all the leakage is located at the eave height, H_e so the pressure difference is given by Eq. (13) with z equal to H_e and the pressure and shelter coefficients are assumed to be the same as the wall below the soffits. The soffit leakage coefficients are estimated as fractions of the total attic distributed leakage coefficient in the soffit or gable. The soffit mass flow rate is then given by Eq. (1).

Localized leaks such as attic vents shown in Fig. 1 provide extra ventilation leakage area in addition to the background distributed leakage. There can be multiple attic vents at different locations on the attic envelope, each with their own leakage coefficient, C_V and flow exponent, n_V . The values for C_V and n_V are user-specified leakage characteristics of each vent. Usually the vent can be assumed to act like an orifice with n_V equal to 0.5. In that case, the vent flow coefficient, C_V can be estimated from the vent area multiplied by the discharge coefficient, K_D . The vent area should be corrected for any blockage effects by insect screens. The pressure coefficient, $C_{p,V}$ and shelter coefficient, $S_{U,V}$ for each vent are assumed to be the same as for the attic surface they are on. The vents are assumed to be small enough that there is no bi-directional flow. The pressure difference across the vent is obtained using Eq. (13) with z equal to H_V , the height of the vent above grade. The vent mass flow rates are then calculated using Eq. (1) with flow exponent, n_V . The direction of mass flow is determined by comparing the value of H_V with the neutral level for the attic surface, $H_{NLa,i}$ on which the vent is located.

As mentioned previously, the ventilation model can include active leakage sites with ventilation fans by incorporating fan performance curves to calculate the mass flow rate through the fan. The fan performance curve can be approximated from the rated fan volume flow rate, Q_{rated} at zero pressure drop across the fan (this is the specification that is usually quoted by the manufacturer) and the maximum pressure that the fan can provide at zero flow rate, ΔP_{rated} . An exhaust fan is

assumed to have a positive value for ΔP_{rated} . The fan performance curve can often be approximated using a power law formulation:

$$\dot{m}_{\text{fan}} = \rho Q_{\text{rated}} \left(\frac{\Delta P_{\text{rated}} + \Delta P_{\text{fan}}}{\Delta P_{\text{rated}}} \right)^{p_{\text{fan}}}, \quad (29)$$

where ρ is evaluated at the attic or outdoor temperature depending on whether the flow is out of or into the attic, respectively. The exponent, p_{fan} depends on the type of fan being used; in this study we have assumed that a centrifugal fan is used with $p_{\text{fan}} = 0.3$. The operating point on the fan performance curve is determined by the pressure across the fan, ΔP_{fan} . The stack and wind pressures across each fan are found by specifying which attic surface the fan is located on and fan height above grade, H_{fan} ; we assume that the inlet and outlet of the fan are located at the same height. The pressure coefficient, $C_{P,\text{fan}}$ and shelter coefficient, $S_{U,\text{fan}}$ are assumed to be the same as the attic surface on which the fan is located.

There can be multiple fans each with their own rated flowrates, Q_{rated} , and rated pressure differences, ΔP_{rated} . The pressure difference across each attic fan, ΔP_{fan} , is given by

$$\Delta P_{\text{fan}} = P_{\text{Ra}} + C_{P,\text{fan}} S_{U,\text{fan}}^2 P_U - H_{\text{fan}} P_{\text{Ta}}. \quad (30)$$

The direction of flow is determined by the sign of the pressure difference. For example, with an exhaust fan if ΔP_{fan} is positive then the exhaust flow rate that the fan delivers will be less than Q_{rated} .

2.5. Calculation of air flows across the interior zone envelope

For the interior zone of the house, the calculation of mass flow rates follows the same development as the attic zone described above. For the distributed leakage of the interior zone, the total distributed leakage flow coefficient, $C_{d,\text{in}}$ and flow exponent, n_{in} can be obtained from fan pressurization tests on the interior zone with all large openings and vents blocked off. The distributed leakage coefficients of the various components of the interior zone such as, walls and ceiling can be expressed as

$$C_{d,\text{in}} = \sum_{i=1}^4 C_{f,i} + \sum_{i=1}^4 C_{w,i} + C_c, \quad (31)$$

where $C_{f,i}$ is the floor level leakage coefficient below wall i , $C_{w,i}$ is the leakage coefficient for wall i and C_c is the ceiling leakage coefficient. Here, we have expressed the floor level leaks separately because the floor and sill plates are usually dominant leakage site in the building envelope. The distributed leakage coefficient for each of the individual components included in Eq. (31) is

estimated by specifying the fraction of total leakage associated with each component.

The mass flow rate associated with the floor level leaks is calculated by first calculating the pressure difference at floor level, H_f from Eq. (11). The pressure and shelter coefficients are assumed to be the same as the wall on which the floor leak is located. The mass flow rate is then calculated from Eq. (1) using the flow exponent, n_{in} . The flow direction is determined by comparing H_f with the neutral level, $H_{\text{NLin},i}$ for the wall surface on which the floor leak is located. The neutral level is given by Eq. (14). If the neutral level is above H_f then there is inflow when T_{in} is greater than the ambient temperature, T_{out} ; if the neutral level is below H_f then there is outflow. For the walls, the flow rate is calculated in the same fashion as the sloped roof surfaces where the leakage is assumed to be uniformly distributed over the surface. On integrating the flow rate over the height of the interior zone, the mass flow rate coming into the zone, $\dot{m}_{w,i,\text{in}}$ is

$$\dot{m}_{w,i,\text{in}} = \frac{\rho_{\text{out}} C_{w,i} \Delta P_{g,i}^{n_{\text{in}}+1}}{H_e (n_{\text{in}} + 1) P_{T\text{in}}}. \quad (32)$$

The limits of integration in Eq. (32) are from $z = 0$ (ground level) to the neutral level, $z = H_{\text{NLin},i}$. The assumption made is that there is no air flow through any distributed leakage in the basement walls below grade. The pressure difference at grade level, $\Delta P_{g,i}$ is given by Eq. (11) with $z = 0$:

$$\Delta P_{g,i} = P_{\text{Rin}} + C_{P,i} S_{U,i}^2 P_U. \quad (33)$$

Similarly, the outflow through the wall, $w_{i,\text{out}}$ is:

$$\dot{m}_{w,i,\text{out}} = \frac{\rho_{\text{in}} C_{w,i} \Delta P_{e,i}^{n_{\text{in}}+1}}{H_e (n_{\text{in}} + 1) P_{T\text{in}}}, \quad (34)$$

where the pressure difference at the top of the wall is obtained from Eq. (11) with z equal to H_e :

$$\Delta P_{e,i} = P_{\text{Rin}} + C_{P,i} S_{U,i}^2 P_U - H_e P_{T\text{in}}. \quad (35)$$

Note that the expression for $\Delta P_{e,i}$ in Eq. (35) pertains to the interior zone and is not the same as that in Eq. (27) which pertains to the attic zone.

For localized leaks such as, fixed vents and active leaks with ventilation fans the procedures for calculating the mass flow rates are identical to those given for the attic zone except Eq. (11) is used for calculating pressure differences and Eq. (14) is used for calculating the neutral level.

The only other leakage flow that needs to be discussed separately for the interior zone is that associated with furnace flues. These localized leaks are usually the largest openings in the building envelope and normally convect hot combustion gases outdoors when the furnace is operating; when the furnace is not operating the flue acts as a large leak convecting indoor air to the

outside. The flue leakage coefficient, C_F , can be calculated from the flue diameter, D_F assuming orifice flow. The values of C_F from experiments by Walker [18] showed that the discharge coefficient of $K_D = 0.6$ should be used in an orifice flow equation. The flow exponent, n_F is close to 0.5. An estimate of the pressure coefficient to be used for furnace flues, $C_{P,F}$, can be found in Haysom and Swinton [19]. Haysom and Swinton measured pressure coefficients at the top of flues with a range of flue caps and found a typical value of -0.5 in a uniform flow. Using this pressure coefficient (which is different from those used on other building leaks) is important because the furnace flue is usually the largest single leakage site on a building. The change in wind velocity with height above grade may be significant for furnace flues that protrude above the reference eaves height, H_e . A corrected $C_{P,F}$ is then given by

$$C_{P,F} = -0.5 \left(\frac{H_F}{H_e} \right)^{2p}, \quad (36)$$

where H_F is the flue top height and p is the power used in the boundary layer wind profile; typically, p is equal to 0.3 for urban surroundings and 0.17 for rural sites [20]. For the flue shelter coefficient, $S_{U,F}$, if the surrounding buildings and other obstacles are below the flue top then it is assumed that $S_{U,F}$ is equal to 1. If the surrounding obstacles are higher than the flue top then the flue is sheltered and $S_{U,F}$ is calculated using Eq. (21). When the furnace is not operating, the pressure difference for the flue is given by Eq. (11)

$$\Delta P_F = P_{Rin} + C_{P,F} S_{U,F}^2 P_U - H_F P_{Tin}. \quad (37)$$

The flue mass flow rate is given by Eq. (1) with a flow exponent of 0.5. When the furnace is operating the temperature of the hot gases in the flue, T_F is used to calculate the density of the hot gases, ρ_F , correct the flow coefficient, C_F according to Eq. (3), and change the driving pressure for flue flow. An extra term $-gH_F(\rho_{in} - \rho_F)$ is added to Eq. (37) to account for the difference in pressure between a flue full of air at temperature T_{in} and hot gases at a flue temperature of T_F . The density difference in this term is expressed in terms of temperature assuming that the hot gases have the same composition as air and are assumed to behave ideally. Thus, the corrected pressure difference for a heated flue is

$$\Delta P_F = P_{Rin} + C_{P,F} S_{U,F}^2 P_U - H_F P_{Tin} - g\rho_{in} H_F \left(\frac{T_F - T_{in}}{T_F} \right). \quad (38)$$

The extra term makes the flue pressure difference more negative and therefore, increases the flow rate through the flue above that of the unheated flue.

2.6. Calculation of interior-attic exchange flow rate

For the interior-attic mass flow rate associated with the ceiling distributed leakage coefficient, C_c , the pressure difference across the ceiling must first be calculated. There are no wind pressures acting on the ceiling except indirectly through the reference pressure differences P_{Rin} for the interior zone and P_{Ra} for the attic zone because the ceiling is completely sheltered from the wind. The pressure difference across the ceiling, ΔP_c is defined as the interior zone pressure minus the attic zone pressure at height, H_e and only includes the difference in attic and interior buoyancy pressures:

$$\Delta P_c = P_{Rin} - P_{Ra} - H_e(P_{Tin} - P_{Ta}). \quad (39)$$

When $T_a = T_{out}$ the buoyancy term is the same as for a house with no attic. When $T_a = T_{in}$ the buoyancy term vanishes and only the difference in internal pressures due to wind forces is acting across the ceiling. The mass flow rate through the ceiling is given by Eq. (1) with ΔP_c and flow exponent, n_{in} . We assume that the ceiling leaks have the same flow exponent as the interior zone of the house.

2.7. Solution of the mass flow rate balance

Once the mass flow rates across a each zone boundary are calculated according to the procedures outlined in Section 2, they are combined in a steady state mass balance for the zone. All of the flow equations contain the unknown reference pressure difference P_{Rin} , for the interior zone and P_{Ra} for the attic zone. We first consider the interior zone. To find P_{Rin} all of the flow equations are combined in a steady state mass balance for the zone:

$$\sum_{i=1}^4 \dot{m}_{f,i} + \sum_{i=1}^4 \dot{m}_{w,i} + \dot{m}_c + \dot{m}_{vent} + \dot{m}_{fan} + \dot{m}_{flue} = 0, \quad (40)$$

where $\dot{m}_{f,i}$ is the mass flow rate through the floor level leak on wall, i , $\dot{m}_{w,i}$ is the mass flow rate through the distributed leakage in wall, i , \dot{m}_c is the exchange mass flow rate through the distributed leakage in the ceiling, \dot{m}_{vent} is the mass flow rate through all vents, \dot{m}_{fan} is the total mass flow rate through all fans, and \dot{m}_{flue} is the mass flow rate through the flue. Note that for the walls, the mass flow rate is separated into inflow and outflow according to Eqs. (32) and (34). The interior and attic zones are coupled through the exchange mass flow rate, \dot{m}_c that is a function of the interior temperature (assumed to be a specified constant value) and the attic temperature. As mentioned previously, the attic air temperature depends on the meteorological conditions, attic ventilation rate, insulation level, and interior-attic

exchange mass flow rate and can be estimated by an attic thermal balance that is coupled with our ventilation model. A combined thermal-ventilation model is beyond the scope of this paper. In Section 3 where we compare measured and predicted attic and interior ventilation rates, we use the measured attic air temperatures as input to the two zone ventilation model.

The mass balance, Eq. (40) is non-linear in P_{Rin} since the flow exponents in Eq. (1) can take on different values between 0.5 and 1 depending on the type of leakage site being considered. A robust iterative bisection technique was adopted because it is unaffected by the non-linearity of the function. This bisection search technique assumes that P_{Rin} equal to 0 for the first iteration and the mass inflow or outflow rates are calculated for each leak. At the next iteration P_{Rin} is chosen to be +1000 Pa if total inflow exceeds total outflow or -1000 Pa if outflow exceeds inflow. These large initial pressure differences mean that even large high pressure fans may be included in the mass balance for the zone. Succeeding iterations use the method of bisection in which P_{Rin} for the next iteration is reduced by half the difference between the last two iterations; thus, the third iteration changes P_{Rin} by ± 500 Pa. The sign of the pressure change is positive if inflow exceeds outflow and negative if outflow is greater than inflow. The limit of solution is determined by the number of iterations. Typically, after 17 iterations the change in P_{Rin} is less than 0.01 Pa, which gives a mass flow imbalance on the order of 0.001 kg/s (or 4 kg/h). This value is much less than the zone ventilation rate. The interior zone ventilation rate is then calculated by summing all the mass flow rates coming into the interior zone.

A similar procedure is carried out for the attic zone, where the steady state mass balance is

$$\sum_{i=1}^4 \dot{m}_{s,i} + \dot{m}_r + \dot{m}_{vent} + \dot{m}_{fan} + \dot{m}_c = 0, \quad (41)$$

where $\dot{m}_{s,i}$ is the mass flow through the distributed leakage in the gable ends or soffits, \dot{m}_r is the mass flow rate through the distributed leakage in the sloped roof surfaces, \dot{m}_{vent} is the total mass flow rate through all vents on the attic envelope, and \dot{m}_{fan} is the flow through all fans located in the attic. The ceiling mass flow rate, \dot{m}_c is the same as the term in Eq. (40) for the interior zone. As with the interior zone, all of the terms in this mass balance equation contain the single unknown, P_{Ra} , the attic to outdoor reference pressure difference. The attic zone is solved using the same bisection technique as the interior zone.

The house and attic zones are coupled by the flow through the ceiling. The interior zone uses the attic reference pressure difference, P_{Ra} to calculate the mass flow through the ceiling. This mass flow is used in the mass flow balance by the attic zone to calculate a new

P_{Ra} . This is also an iterative procedure that continues until the change in mass flow through the ceiling from iteration to iteration is less than 0.00001 kg/s. The convergence criteria yields an error in the ceiling flow rate that is typically about 0.01% of the total interior zone infiltration flow rate.

3. Validation of the attic-interior infiltration model

In this section the two zone ventilation model will be validated by comparing their predictions to measured values. The measurements, made at the Alberta Home Heating Research Facility, have been described in Walker and Forest [1]. The ventilation model will be verified using measured attic air temperature as this is required to calculate the air density. Future work will involve combining the ventilation model with an attic thermal balance model; the focus of this paper is on the ventilation model. The difference between predictions and measurements will be expressed using the following four error estimates: *mean* error is the mean of the differences between each pair of measured and predicted data points, *absolute* error is the mean of the absolute value of the differences between each pair of measured and predicted data points, *percent* error is the mean of the percentage differences between each pair of measured and predicted data points, and *absolute percent* error is the mean of the absolute percentage differences between each pair of measured and predicted data points.

We first consider the prediction and measured ventilation rates for the attic. The ventilation model predictions of the total attic ventilation rate were verified by comparing model predictions to measured data from the two attics described by Walker and Forest [1]. Both attics have identical gable end configurations as shown in Fig. 1 with attic floor dimensions of 6.7 × 7.3 m; the eaves add another 1.1 m to the width of the attic. The sloped roof surfaces have a 3:1 pitch and are raised 0.67 m above the attic floor to accommodate different levels of ceiling insulation. The roof surfaces are sheathed with 9.5 mm exterior plywood and 210# brown asphalt shingles. The roof trusses are made of 38 mm by 89 mm spruce lumber and are spaced at a standard 61 cm interval. The ceiling consists of 12.7 mm drywall, 0.1 mm polyethylene vapor retarder, and 89 mm glass fibre batt insulation. The total enclosed volume of the attic is estimated to be 61 m³. One attic is constructed as a “tight” attic with no vents or soffits (attic 5) while the other attic has continuous soffits along both eaves and two flush-mounted vents one on each sloped roof surface (attic 6). The gross open area of the soffits was estimated to be 0.040 m² while each vent had a gross area of 0.036 m² which was reduced by the presence of a screen. Fan pressurization tests showed

that the tight attic had a background leakage area, $A_{L4} = 0.0456 \text{ m}^2$ while the other attic had a background leakage area with all vents sealed off, $A_{L4} = 0.154 \text{ m}^2$. The measured flow exponents for attic 5 and 6 were 0.707 and 0.597, respectively. The two attics are a good test of the ventilation model as they represent possible extremes for typical attic construction.

In order to make predictions of ventilation rates in the two attics assumptions were made about the leakage distribution over the attic envelope. The assumed distribution of this leakage is summarized in Table 3, together with the additional vents for attic 6. The distribution was estimated by visual inspection by the first author. In Table 3 the percentages are the fractions of background leakage estimated to be at the specified locations. The smallest amount of leakage considered in these estimates is 5% because it was unreasonable to make a more accurate estimate without detailed component leakage measurements in the attics. The total ventilation rate predicted by the attic ventilation model was relatively insensitive to the leakage distribution estimates provided that extreme values were not used e.g. all of the leakage at one location. Moving 5% of leakage between different locations changed the total predicted ventilation rate by less than 5%. The numbered surfaces in Table 3 have the same numbering scheme as shown in Fig. 1.

The ventilation model also computes the house ventilation rates and the flow between the house and attic through the ceiling. The interior zones of the two

houses are identical with no vents or other large openings present during the test period. The distribution of house leakage used to perform these calculations is summarized in Table 4. As with the attic, these leakage distributions are estimated by inspection. The exception is the fraction of leakage in the ceiling which is calculated from the difference in leakage areas found from the pressurization tests for the house with the ceiling holes open and covered. The wall and floor level leakage is assumed to be equally distributed over the four sides of the building.

The other inputs to the ventilation model are wind speed, wind direction (to calculate pressure coefficients and wind shelter), and house, attic and outdoor temperatures. As mentioned above, the measured attic temperature was used for the data comparisons.

3.1. Stack and wind induced attic ventilation rates

To better identify which parts of the ventilation model may be contributing to differences between measured and predicted ventilation rates, the model predictions have been compared with both stack effect and wind effect dominated ventilation rates. The attic ventilation rate was not a strong function of the attic temperature as shown by Figs. 7 and 8, for attics 5 and 6, respectively. In these figures the maximum temperature difference (stack) induced ventilation rate was only about 20% of that due to wind effects as shown in Figs. 9 and 10. In Figs. 7 and 8 the measured data has

Table 3
Assumed percentage distribution of background leakage area for attics 5 and 6 and location and size of attic 6 roof vents

Surface or point on attic envelope	Attic 5		Attic 6	
	% or area (m^2)	Height above grade (m)	% or area (m^2)	Height above grade (m)
Eaves on roof surface 1	25%	3	45%	3
Eaves on roof surface 2	25%	3	45%	3
Gable—surface 3	5%	distributed	0	—
Gable—surface 4	5%	distributed	0	—
Roof surface 1	20%	distributed	5%	distributed
Roof surface 2	20%	distributed	5%	distributed
Vents on roof surface 1	0	—	0.036 m^2	4.5
Vents on roof surface 2	0	—	0.036 m^2	4.5
Roof peak	0	5	0 m^2	5

Table 4
Assumed interior zone percentage leakage distributions and locations for house 5 and 6

Location on building envelope	House 5		House 6	
	%	Height above grade (m)	%	Height above grade (m)
Floor level	20	0.6	15	0.6
Ceiling	15	3	15	3
Walls	65	distributed	70	distributed

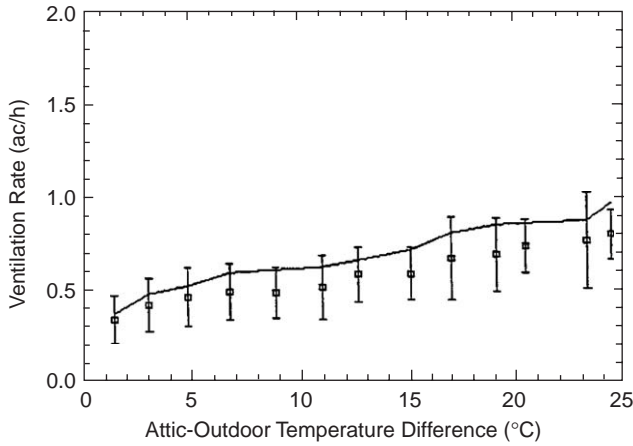


Fig. 7. Temperature difference induced ventilation rates for attic 5 for wind speeds less than 2 m/s (589 hourly averaged data points) showing mean and standard deviation of binned measured data. The solid line connects the mean predicted values for each temperature difference bin.

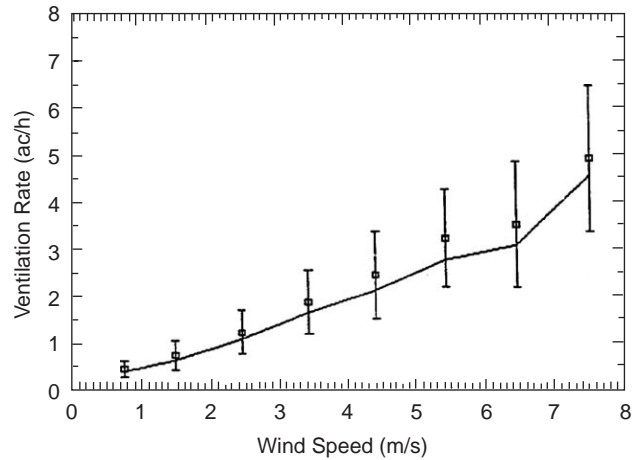


Fig. 9. Measured mean and standard deviations ventilation rates for attic 5 (3758 hourly averaged data points) for all wind directions and temperature differences. The solid line connects the mean predicted values for each wind speed bin.

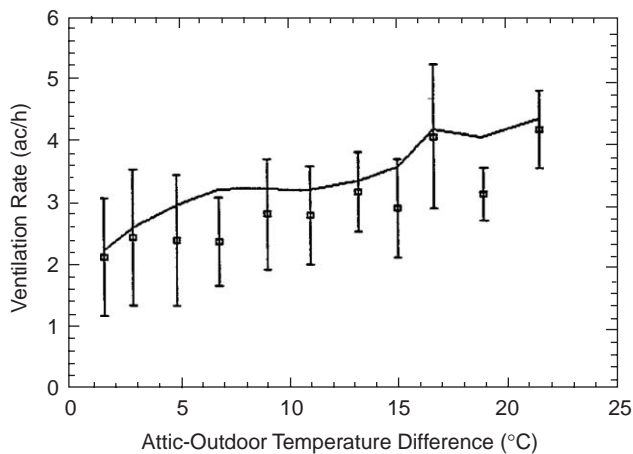


Fig. 8. Temperature difference induced ventilation rates for attic 6 for wind speeds less than 2 m/s (464 hourly averaged data points) showing mean and standard deviation of binned measured data. The solid line connects the mean predicted values for each temperature difference bin.

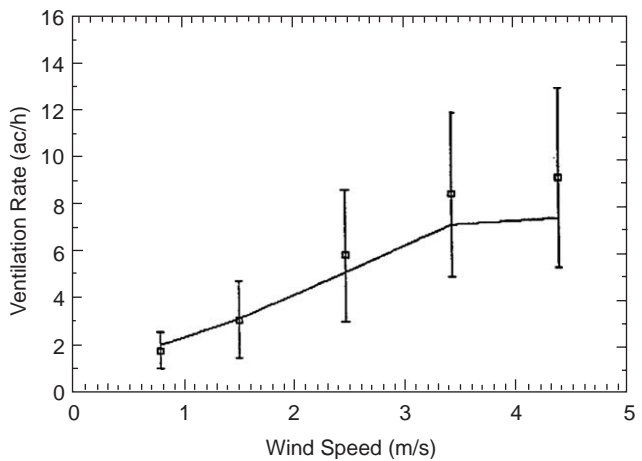


Fig. 10. Measured mean and standard deviations ventilation rates for attic 6 (3522 hourly averaged data points) for all wind directions and temperature differences. The solid line connects the mean predicted values for each wind speed bin.

been sorted for wind speeds less than 2 m/s (to remove the higher wind speed effects) and binned every 2 °C of attic to outdoor temperature difference. The square indicates the mean value of hourly data in the bin and the error bars show one standard deviation of the measured data. A solid line is used to connect the means of the predicted ventilation rates that are also averaged for each bin. Figs. 7 and 8 show that the model tends to over predict these stack driven ventilation rates. For attic 5 the mean error is 0.07 ac/h (19%) and for attic 6 the mean error is 0.34 ac/h (21%). The percentage errors are large for the stack driven ventilation rates because the ventilation rates are low. At wind speeds less than 2 m/s the following Figs. 9 and 10 show that the wind

produces flow rates that are about the same as those for the stack effect only in Figs. 7 and 8. Because the wind effect tends to be under predicted the inclusion of some wind effect does not account for the systematic over prediction of stack effect ventilation rates. The wind produces maximum ventilation rates that are about five times greater than for stack effect which would reduce the percentage errors for the combined stack and wind driven ventilation.

Figs. 9 and 10 show attic zone predictions compared to measured values for attic 5 and attic 6 for all temperatures. The maximum wind speed in Fig. 10 for attic 6 was limited to 5 m/s because at 6 m/s (about 20 ac/h) and higher the measured values were unreliable

due to incomplete tracer gas mixing. In order to compare measured values and predictions more clearly, the measured data was binned every 1 m/s of wind speed. The ventilation rates were predicted for each hour (3758 h for Fig. 9 and 3522 h for Fig. 10). Their mean values at the mean wind speed for each hour were connected by a straight line in the figures. The trend in increasing ventilation rate with wind speed shown by the measured values was followed by the model predictions with a general tendency towards under prediction. For attic 5 the mean error was -0.017 ac/h (-9.3%) and for attic 6 the mean error is -0.5 ac/h ($+4.3\%$). Most of this under prediction occurred when the wind blew along the row of houses (as will be shown later in this section). The attic 6 mean percentage error was positive because its over predictions occurred at lower ventilation rates where the percentage over prediction was high but the mean error in ventilation rate was relatively small. Considering the uncertainty in pressure coefficients, wind shelter and leakage distributions these errors were about as small as could be reasonably expected. The values of these input parameters were not adjusted to reduce the errors. The model would then have been fitted to the measured data for the test houses and this procedure would not have validated the model in a general sense.

3.2. Effect of wind direction on attic ventilation rates

The wind direction has a very strong effect on ventilation rate for a house in a closely spaced row because it changes the wind pressure coefficients and wind shelter. To test if the model has the correct variation of pressure coefficient and shelter the measured and calculated ventilation rates for attic 6 are shown in Figs. 11 and 12, respectively. Both figures illustrate the same trends with lower ventilation rates for east and west winds (90° and 270°) than for north and south winds (0° and 180°). The large spread of data for a given wind direction is because a range of wind speeds and temperature differences are present. In addition, using an hourly averaged wind direction produces scatter with respect to wind direction in the results because the wind direction may change during the hour. The lower ventilation rates for a given direction correspond to lower wind speeds and temperature differences and the high ventilation rates to high wind speeds and temperature differences. There is less scatter in the predicted data because the measured data has included all the hourly variation in parameters such as wind speed, wind direction and temperatures that are not included in the hourly averages entered in the model.

To better observe the model performance, the measured and predicted data were binned every 22.5° to provide 16 wind direction bins. The data were then normalized by dividing by U^{2n} to remove the effects of

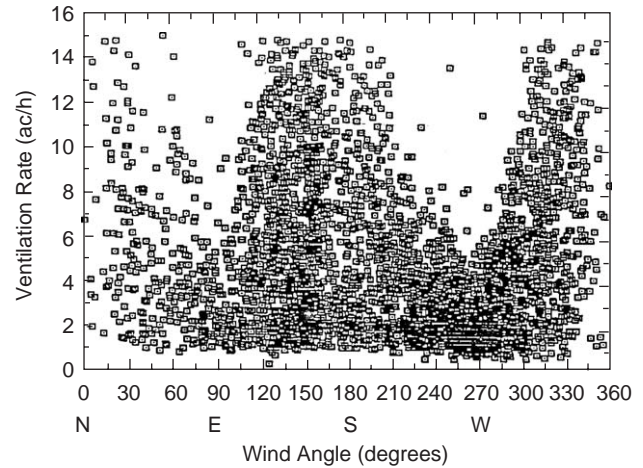


Fig. 11. Variation of measured hourly averaged ventilation rates with wind direction for attic 6 (3522 hourly averaged data points). Compare with Fig. 12.

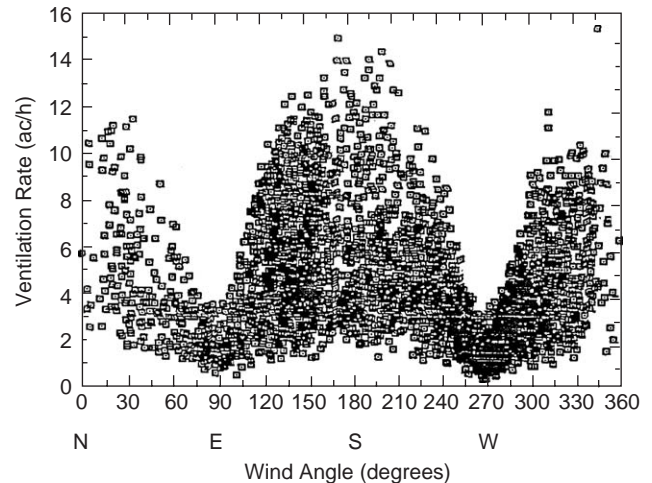


Fig. 12. Variation of predicted hourly averaged ventilation rates with wind direction for attic 6 (3522 hourly averaged data points). Compare with Fig. 11.

changing wind speed. In each bin the data were averaged and the measured standard deviation was calculated. A further normalization was carried out by dividing all the binned averages by the mean ventilation rate from the bin for south winds. This south wind direction bin was chosen because the test houses were completely exposed to winds from the south and there should be no wind shelter for that direction. Figs. 13 and 14 show the results of this procedure for attic 5 and attic 6, respectively. For attic 5 the normalized air exchange rates are about 50% less for east and west winds than for north and south winds due to the sheltering effects of the neighboring buildings. For attic 6 the sheltering effect is asymmetric with a reduction of almost 60% for west winds and only 40% for east winds. This is because attic 6 is sheltered by the row of houses for west winds

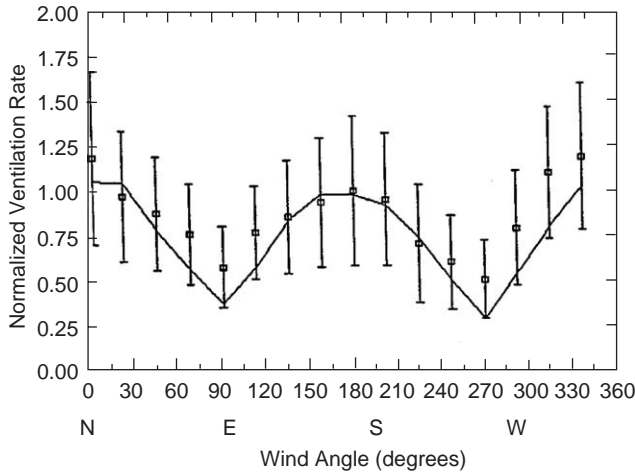


Fig. 13. Comparison of predicted and measured normalized ventilation rates as a function of wind direction for attic 5 (3758 hourly averaged data points). Measured data shown as a binned data point with standard deviation and solid line joins the mean predicted values for each wind direction bin.

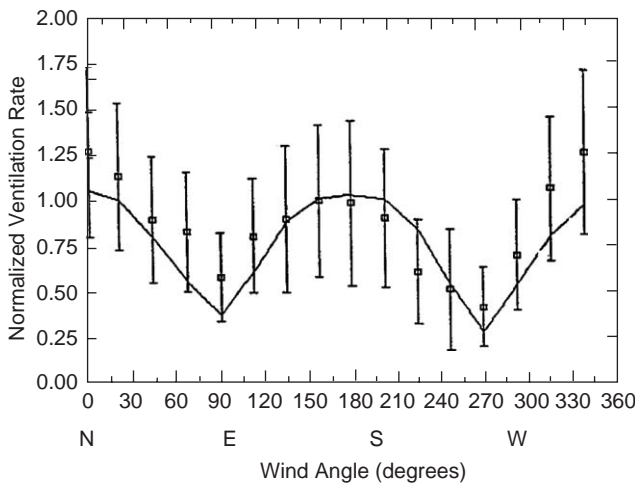


Fig. 14. Comparison of predicted and measured normalized ventilation rates as a function of wind direction for attic 6 (3522 hourly averaged data points). Measured data shown as a binned data point with standard deviation and solid line joins the mean predicted values for each wind direction bin.

but for east winds only partial shelter is provided by a rectangular vertical barrier 3.7m high and the same width as the houses. The data shows that this sheltering barrier does not have the same shelter effect as an upwind house. This is for two reasons: firstly, the wall only extends 0.7m above eaves height of the house and leaves the rest of the attic exposed: secondly, the flow pattern around the wall is different from that around a house due to flow separation at the sheltering wall edges.

The model follows the trends in normalized air exchange with wind direction and for both attics the largest error is an under prediction of about 25% when winds are from the east or west. This error is due to the

Table 5
Mean and percentage errors of predicted ventilation rates for attics 5 and 6

	Attic 5 mean error, ac/h (%)	Attic 6 mean error, ac/h (%)
For stack dominated ventilation	0.07 (19)	0.34 (21)
For wind dominated ventilation	-0.02 (-9.3)	-0.5 (4.3)
All wind directions		
North winds only	-0.04 (2.2)	-1.7 (-14.1)
South winds only	0.15 (14.2)	0.08 (18.9)
East winds only	-0.24 (-25.8)	-1.50 (-27.1)
West winds only	-0.28 (-28.8)	-0.75 (-17.1)

combination of errors in estimating shelter factors and the error associated with assuming constant pressure coefficients over the surfaces of the attic. The shelter factors applied to the attics were initially developed for house walls. The attics are closer to the undisturbed air flow over the houses and may experience less shelter. Also, in the real flow over the attic there will be a strong spatial variation in the pressure coefficients that will create pressure differences and flow rates not accounted for in our ventilation model. The model mean and percentage errors are summarized in Table 5 including the variation of error with wind angle.

3.3. Interior zone ventilation rates

Although this study concentrates on attic ventilation rates, the house interior zone ventilation rates were also calculated. The house ventilation rates are important not only in their own right for control of indoor air quality but also because the interior zone reference pressure difference is combined with the reference pressure difference in the attic to determine the leakage flow rate through the ceiling. The house ventilation rates will not be discussed in detail here but a few results will be given to show that the ventilation model makes good predictions of house ventilation rates. A more thorough investigation of house ventilation rate predictions by the ventilation model used here is presented by Wilson and Walker [21,22]. The house ventilation rates in air changes per hour were based on the volume of the house (220m³ for the houses tested here).

Figs. 15 and 16 are typical results found by Wilson and Walker [16] for house 5 for stack and wind dominated ventilation. In Fig. 15 data has been sorted for maximum wind speeds of 2m/s to look at stack effect only. The mean error for the data shown in Fig. 15 is 0.005 ac/h (6.4%). In Fig. 16 the data has been selected for wind speeds greater than 2m/s to look at wind dominated ventilation (all wind directions are included). The error for the wind dominated ventilation rates shown in Fig. 16 is -0.003 ac/h (3%). In both

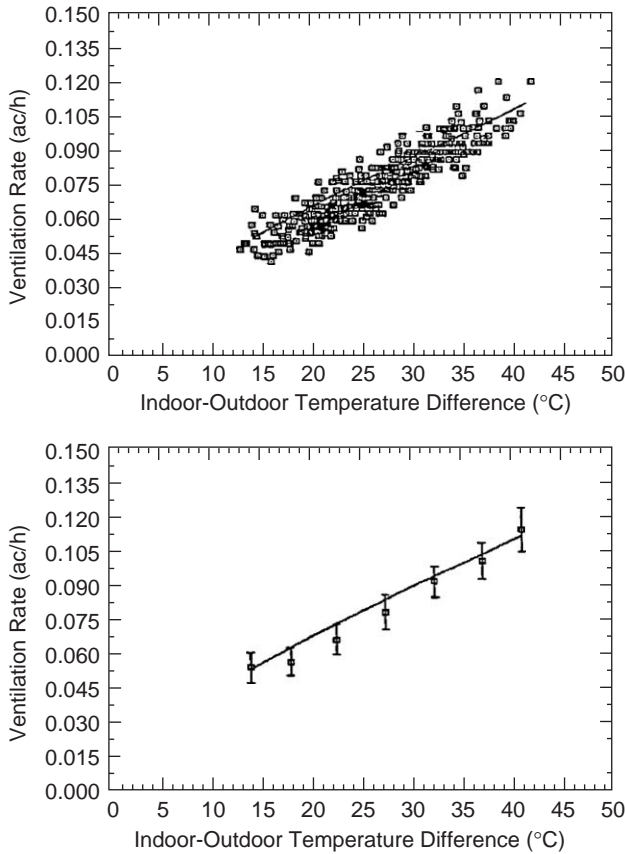


Fig. 15. Comparison of measured and predicted stack effect ventilation rates for house 5 for wind speeds less than 2 m/s (461 hourly averaged data points). Upper plot shows all measured data and lower plot shows binned average values and standard deviations.

Figs. 15 and 16, the upper figure shows the individual measured data points and the lower figure binned measured and predicted data.

3.4. Interior—attic exchange rates

The leakage flow rate through the ceiling is an important quantity because this flow convects room temperature air and moisture into the attic. The ventilation model calculates this flow based on the leakage area attributed to the ceiling and the pressure differences between the house and attic. The ceiling leakage areas for house 5 and 6 were measured to be 0.0012 and 0.0010 m², respectively. The measured interior-attic exchange rates were calculated based on the concentration of SF₆ in the attic described by Walker and Forest [1] and are expressed as attic air changes per hour using an attic volume of 61 m³. It was found that the house to attic exchange rate depends most strongly on the temperature difference between the house and the attic. The effect of wind speed is small because the mean pressures in both zones caused by the wind are approximately equal. To reduce scatter the data was sorted for wind speeds less than 2 m/s. Model

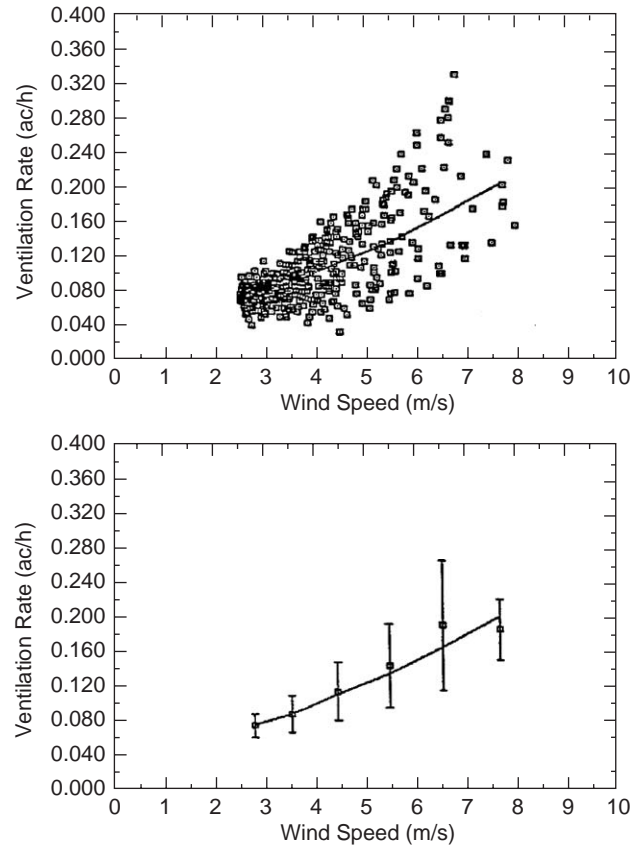


Fig. 16. Comparison of measured and predicted stack effect ventilation rates for house 5 for wind speeds greater than 2 m/s (432 hourly averaged data points). Upper plot shows all measured data and lower plot shows binned average values and standard deviations.

predictions for attics 5 and 6 are compared with measured data in Figs. 17 and 18. These figures show good agreement between measured and predicted values considering how small these exchange rates are. The standard deviation error in hourly means for attic 5 is -0.015 ac/h (4.5%) and for attic 6 it is 0.0014 ac/h (14.3%). For both attics the peak exchange is about 0.25 ac/h which is only a few percent of the total attic ventilation rate. Typically the room to attic exchange is about 10% of the total for attic 5 and only 2% of the total for attic 6.

4. Summary and conclusions

The two zone ventilation model developed for this study has been verified by comparing their predictions to measured hourly averaged data. The validation procedure has illustrated that a large amount of measured data is required in order to isolate individual parameters, e.g. selecting wind speeds below 2 m/s to look at temperature difference driven ventilation rates. The following sections discuss typical differences between measure and predicted values.

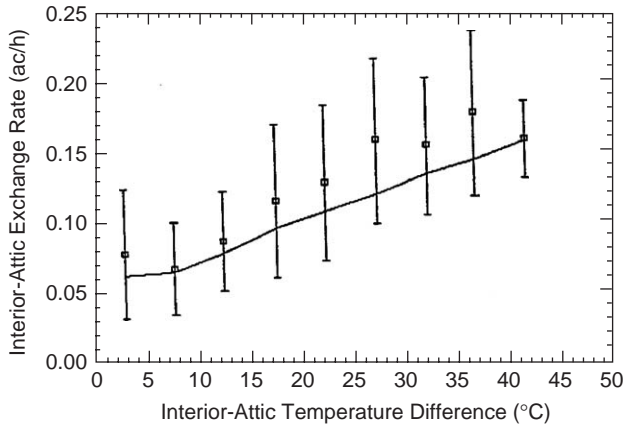


Fig. 17. Comparison of measured and predicted interior-attic exchange rates for attic 5 for wind speeds less than 2 m/s (990 hourly averaged data points). Measured data shown as a binned data point with standard deviation and solid line joins the mean predicted values for each interior-attic temperature difference bin. Exchange rates are based on an attic volume of 61 m³.

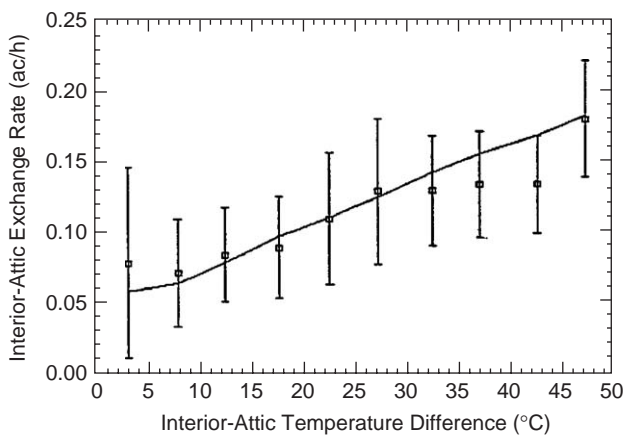


Fig. 18. Comparison of measured and predicted interior-attic exchange rates for attic 6 for wind speeds less than 2 m/s (722 hourly averaged data points). Measured data shown as a binned data point with standard deviation and solid line joins the mean predicted values for each interior-attic temperature difference bin. Exchange rates are based on an attic volume of 61 m³.

The attic ventilation rates were found to be a weak function of the attic temperature. The maximum stack driven ventilation rates were only 20% of the wind driven ventilation rates. The typical mean error for stack driven attic ventilation rates is about 20%. The mean errors for the more dominant wind driven ventilation are less, typically 5–10% of the measured values. Because the wind driven ventilation is much larger than the stack driven ventilation the errors for wind driven ventilation are a better indicator of the overall ventilation model performance. The absolute errors are much larger, typically 20–30%. The mean errors are systematic errors due to uncertainty in leakage distribution,

assumed wall averaged pressure coefficients and shelter factors. The absolute errors include the variability of ventilation rate during the hour due to changing wind speed, wind direction and temperatures. Wind direction was found to create up to a factor of 300% change in ventilation rate due to shelter effects for the row of houses. The results showed that the greatest under prediction of ventilation rates occurred for winds blowing along the row of houses, when shelter effects are the most important. The mean errors were about –15% to –30% for these wind directions. This under prediction is due to a combination of the following factors: The shelter factors applied to the attics were developed for the houses but the attics are closer to the undisturbed air flow over the houses and thus may experience less shelter. The assumption of uniform pressure coefficients over large areas of the attic is critical when the wind blows along the row of houses and all the attic leaks have the same pressure coefficient. In the real three-dimensional flow there are local variations in pressure coefficient that are not accounted for in this model. These local changes in pressure coefficient would create pressure differences across the attic leaks resulting in greater attic ventilation rates.

The flow of air from the house to the attic is very important for the heat and moisture transport. The magnitudes of the flow through the ceiling are small compared with the overall attic ventilation rates. The measured and predicted values indicate that the room to attic exchange is about 10% of the total ventilation rate for attic 5 and only 2% in attic 6. The maximum exchange rate is about 0.25 ac/h in both attics. Considering what a small percentage of the total flow the house to attic exchange is, the ventilation model predicts the exchange very well with mean errors of 0.015 ac/h (5%) for attic 5 and 0.0014 (15%) for attic 6. For attic 6 the mean absolute error is smaller than in attic 5, but the mean percentage error is larger. This is because the over predictions for attic 6 occur when the flow rate is low, which results in large positive percentage errors.

The two zone ventilation model for houses with attics has been presented. The model has been developed to use information that might reasonably be known about a building. The validation procedure has shown that the simplifying assumptions made in order to make the models reasonable to use do not result in unrealistic predictions. Most of the time the model predictions are as good as can be determined using field measurement techniques.

Acknowledgements

Funding for this work was provided through Canada Mortgage and Housing Corporation and NSERC. The

authors would like to acknowledge the assistance of Wayne Pittman and Mark Ackerman with the ventilation measurements at the Alberta Home Heating Research Facility.

References

- [1] Walker IS, Forest TW. Field measurements of ventilation rates in flat ceiling attics. *Building and Environment* 1995;30(3):333–47.
- [2] Sherman MH, Grimsrud DT. The Measurement of infiltration using fan pressurization and weather data. Report # LBL-10852, Lawrence Berkeley Laboratories, University of California, 1980.
- [3] Walker IS, Wilson DJ. AIM-2 The Alberta Infiltration Model. Department of Mechanical Engineering Report #71, University of Alberta, Edmonton, Canada, 1990.
- [4] Walker IS, Wilson DJ. Including Furnace Flue Leakage in a Simple Air Infiltration Model. *Air Infiltration Review* 11(4), September 1990, AIVC, Coventry, UK: 4–8, 1990.
- [5] Walker IS, Wilson DJ. Evaluating models for superposition of wind and stack effect in air infiltration. *Building and Environment* 1993;28(2):201–10.
- [6] Forest TW, Walker IS. Attic ventilation model. Proceedings of ASHRAE/DOE/BTECC Thermal Performance of the Exterior Envelopes of Buildings V, Clearwater Beach, FL, December. 1992. p. 399–408.
- [7] Walker IS, Forest TW, Wilson DJ. A simple calculation method for attic ventilation rates. Proceedings of the 16th AIVC Conference, Palm Springs, USA, September, 1995. p. 222–31.
- [8] Feustal HE, Raynor-Hoosen A. Fundamentals of the Multizone Model—COMIS. Air Infiltration and Ventilation Centre Technical Note 29, AIVC, Coventry, UK, 1990.
- [9] Dale JD, Ackerman MY. The thermal performance of a radiant panel floor-heating system. *ASHRAE Transactions* 1993;99(1): 24–34.
- [10] Kiel DE, Wilson DJ, Sherman MH. Air leakage flow correlations for varying house construction types. *ASHRAE Transactions* 1985;91(2):560–75.
- [11] Walker IS, Wilson DJ. Practical methods for improving estimates of natural ventilation rates. Proceedings of the 15th AIVC Conference, Buxton, UK, 1994; p. 517–25.
- [12] Walker IS, Wilson DJ. Wind shadow shelter model. *ASHRAE Journal of HVAC&R Research* 1995;2(4):265–83.
- [13] Akins RE, Peterka JA, Cermak JE. Averaged pressure coefficients for rectangular buildings. *Wind Engineering* 1, Proceedings of the Fifth International Conference on Wind Engineering, 1979, 369–380.
- [14] Wiren BG. Effects of surrounding buildings on wind pressure distributions and ventilation losses for single family houses : Parts 1 and 2. National Swedish Institute for Building Research Report M85: 19, 1985.
- [15] Liddament MW. Air infiltration calculation techniques—an applications guide. Air Infiltration and Ventilation Centre, Coventry, UK, 1986.
- [16] Wilson DJ, Walker IS. Passive Ventilation to Maintain Indoor Air Quality. Department of Mechanical Engineering Report #81, University of Alberta, Edmonton, Canada, 1991.
- [17] Wilson DJ. Flow patterns over flat-roofed buildings and application to exhaust stack design. *ASHRAE Transactions* 1979;85(2):284–95.
- [18] Walker IS. Single zone air infiltration modelling. M.Sc. Thesis, Department of Mechanical Engineering, University of Alberta, Edmonton, Canada, 1989.
- [19] Haysom JC, Swinton MC. The influence of termination configuration on the flow performance of flues. Canada Mortgage and Housing Corporation Report, Scanada Consultants Limited, 1987.
- [20] Irwin JS. A theoretical variation of the wind profile power law exponent as a function of surface roughness and stability. *Atmospheric Environment* 1979;13:191–4.
- [21] Wilson DJ, Walker IS. Wind shelter effects on a row of houses. Proceedings of the 12th AIVC Conference, Ottawa, Canada, 1991.
- [22] Wilson DJ, Walker IS. Feasibility of passive ventilation by constant area vents to maintain indoor air quality. Proceedings of the Indoor Air Quality '92, ASHRAE/ACGIH/AIHA Conference, San Francisco, October 1992.